THREE-DIMENSIONAL VISUALIZATION AND MORPHOMETRY OF SMALL AIRWAYS FROM MICROFOCAL X-RAY COMPUTED TOMOGRAPY

Toshihiro SERA (1,5), Hideki FUJIOKA (2), Hideo YOKOTA (3), Akitake MAKINOUCHI (3), Ryutaro HIMENO (3), Robert C. SCHROTER (4) and Kazuo TANISHITA (1)

(1) Center for Life Science and Technology, Keio Univ., Yokohama, JAPAN

(2) Biomedical Engineering Department, University of Michigan, Ann Arbor, MI

(3) Advanced Computed Center, Institute of Physical and Chemical Research (RIKEN), Wako, JAPAN

(4) Department of Bioengineering, Imperial College of Science, Technology and Medicine, London, UK

(5) Life & Environmental Science Division, Japan Synchrotron Radiation Research Institute (JASRI), Sayo, JAPAN

INTRODUCTION

Small airways consist of tapered, curved, branching tubes of a range of length and diameter. Important respiratory functions, such as airway dynamics, airflow structure, surfactant transport, and particle deposition occur in the small airways. Consequently, airway morphometry has been extensively studied [1-4]. However, previous techniques, such as the fixed preparation methods, deform the geometry during sample preparation. Moreover, small airways are flexible tissue, and thus their geometry varies markedly during respiration. Previously we developed a two-step method to visualize small airways in detail by staining the lung tissue with a radiopaque solution and then visualizing the tissue with a cone-beam microfocal X-ray CT system (micro-CT), without dehydration and fixation of the tissue [5]. In this study, we visualized and analyzed the three-dimensional morphometry of small airways using our proposed technique.

MATERIALS AND METHOD

Animal Preparation

After male fourteen Wister rats (300 ± 30 g) were anesthetized with pentobarmital sodium (50 mg/kg ip), they were exsanguinated and cardiac arrest was induced by 0.2 g/ml KCl solution. The water mixed this a radiopaque media, Sodium diatrizoate (Sigma Chemical, St Louis, MO) in the quantity 0.8 g/ml, was induced into an inferior vena cava. After the solution was stained to lung tissue for 1 h, the lungs were removed.

Imaging

The small airways were visualized by a microfocal X-ray CT system (MCT-CB100MF, Hitachi Medical Corp., Japan, Tokyo). The Resolution was 480 × 480 pixel and 1 voxel size was 14 μm. In one rotation, the number of slice images was obtained 200 images. The excised rat lung induced by the radiopaque solution was placed into a Plexiglas cylinder in. It was mounted on the rotation stage, and it took 2.5 min to rotate around 360°.

Measurements

To investigate the morphometry of the small airways, we identified the cross-sections of the small airways using the threshold method from micro-CT images and then analyzed using the three-dimensional thinning algorithm described by Toriwaki ea al. [6].

The airway has approximately the shape of a hollow cylinder network and we calculated the diameter D, length L, branching angle α, and gravity angle β between the gravity direction and airway vector from airways skeletons. In this study, β was analyzed the only downward airways to distal side.

RESULTS AND DISCUSSION

Fig. 1 is a representative micro-CT image (1 pixel is 16 μm) and three-dimensional reconstruction images using an isosurface approach (Diamter range: 300 μm ~ 170 μm). Fig.1A shows not only small airways but also alveoli. The pixel intensity of the lung tissue was stronger than that of the small-airway lumens. The regions of strongest image intensity indicate airway walls and pulmonary vessels.

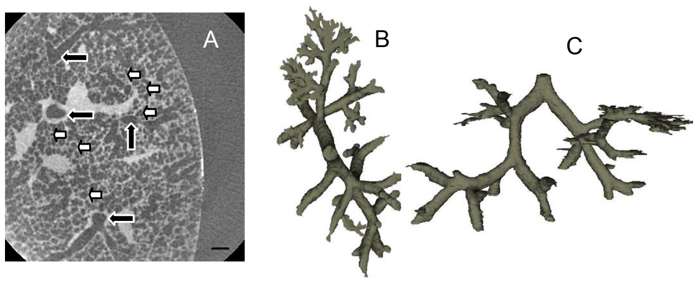

Fig. 1 The Representative micro-CT image (A, Black arrows: small airways and white arrows: alveoli. Bar: 500 μm) and three-dimensional structures (B (top view), C (side view))

Fig. 2 shows the original outlines of the cross-sections and the middle lines, and it was apparent that the middle lines agreed with the outlines. In this study, the thinning algorithm is two-step to make the

Euclidean distance transformation and then check deletability of the points in sequence that the Euclidean distance is small. Using this algorithm the middle lines were correctly calculated without changing the topology of the airways even if the original images were shifted and rotated from the vertical direction.

Using these middle lines we calculated the average diameter D and average length L as a function of the Weibel's airway generation Z ranging from 8 to 16 in Fig. 4. The average diameter and length decreased by an exponential function like Weibel data and was fitted to the Eq. (1) and (2).

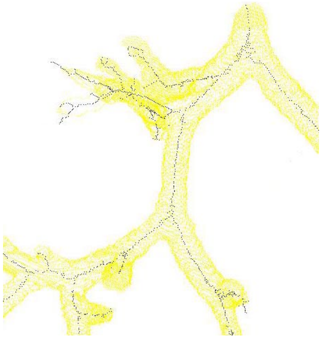

Fig. 2 The superimposed three-dimensional structure and its skeleton. (Black lines)

$$D(Z) = 1.1104 \cdot 2^{-0.1777Z} \quad (1)$$

$$L(Z) = 1.7015 \cdot e^{-0.0851Z} \quad (2)$$

The average diameter ratio (daughter diameter / parent diameter) in small airways was 0.89 and the average ratio length to diameter (L/D) was 2.26 ranging from 2.02 to 2.63.

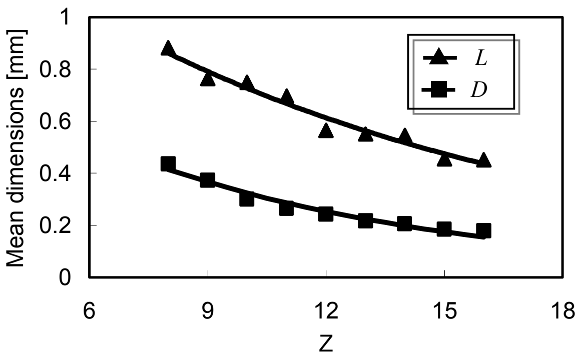

Fig. 3 The average diameter *D* (square) and average length *L* (triangle) as a function of the airway generation *Z*.

The branching angle α and gravity angle β were approximately constant at 133.3 ± 23.8° and 63.9 ± 13.2° over the generations studied It is well known that the airways branch asymmetrically and therefore the asymmetry of the bifurcation *As* was defined as follows.

$$\mathrm{As} = \alpha 1 / \alpha 2 \, (\alpha 1, \alpha 2 \subseteq \alpha) \quad (3)$$

$\alpha 2$ was defined as the pair branching angle of $\alpha 1$, and $\alpha 1$ was major and $\alpha 2$ was minor ($\alpha 1 > \alpha 2$). *As* decreased with Z, consistent with the geometry data presented by Phalen et al. [2]. And *As* proportionally decreased with $\alpha 2$ and was linearly fitted to the Eq. (4).

$$As = -0.0131 \cdot \alpha 2 + 2.8791 \quad (4)$$

Eq. (3) indicated that one branching angle ($\alpha 1$) decided the other pair branching angle ($\alpha 2$) and in the case of the symmetric bifurcation ($\alpha 1 = \alpha 2$) the branching angle was approximately 140°.

This method does not require dehydration and fixation to visualize small airways in detail in "near" physiological conditions, and so we visualized the same airways in various lung volumes (Fig. 4). Fig. 5 shows the diameter increment as a function of the default diameter at FRC (functional residual capacity). The diameter of small airways expanded about 1.1 ~1.7 times at tidal volume and 1.2 ~ 2.5 times at TLC (total lung capacity) in comparison with at FRC. For many years the lung compliance has been evaluated from the macroscopic viewpoint and described particularly in terms of the pressure – volume curve; however using this method compliance can be investigated at the microscopic local level of small airways and alveoli. Furthermore this morphometry change during respiration will open the way to new research of the pulmonary dynamics.

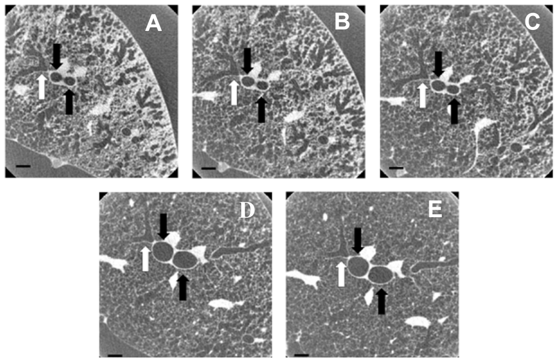

Fig. 4 The micro-CT images of the same airways in various lung volumes. (A: 3ml (FRC), B: 5ml, C: 7ml, D: 9ml, and E: 11ml (TLC), Bar: 500 µm)

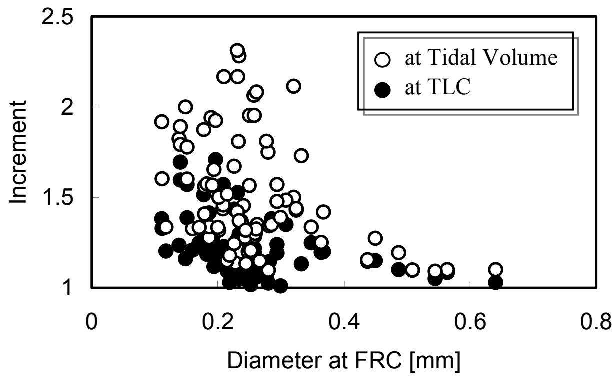

Fig. 5 The diameter increment at tidal volume and TLC as a function of the default diameter at FRC

REFERENCE

1. Weibel ER., 1963. *Morphometry of the Human lung*, New York:
2. Horsfield K., Dart G., Olson DE., Filly GF., Cumming G., 1971. "Models of the human bronchial tree." Journal of Applied Physiology, 31(2), 207-217.
3. Phalen RF., Yeh HC., Schum GM,. Raabe OG.., 1978. "Application of an idealized model to morphometry of the mammalian tracheobronchial tree." Anatomical Record, 190(2), 167-76.
4. Sauret, V., Halson, PM., Brown, IW., Flemming JS., and Baily AG., 2002. "Study of the three-dimensional geometry of the central conducting airways in man using computed tomographic (CT) images." Journal of Anatomy, 200, 123-134.
5. Sera T, Fujioka H, Yokota H, et al., 2002, "New method of three-dimensional imaging of small airways in rats with x-ray micro-CT." Proceeding of IV World Congress of Biomechanics, Calgary.
6. Toriwaki, J., and Mori K., 2001. "Distance transformation and skeletonization of 3D pictures and their applications to medical images." In: Bertrand G., Imiya A., Klette R. (Eds.), Digital and Image Geometry, Springer, Tokyo, pp.412-428.